Calculation of the p p $\rightarrow t\bar{t}$ Higgs cross section at the LHC and potential background analysis

DESY SUMMER STUDENT PROGRAM 2007

Angeliki Koutsoukou- Argyraki *

ABSTRACT

In this report we present the cross section values for some top pair production processes at the LHC. The Feynman diagrams for the gluon subprocesses as well as some histograms for the processes $pp \rightarrow t\bar{t}$ *and* $pp \rightarrow t\bar{t}$ *jet are also presented.We perform cross section calculations at various factorization scales .We study the* $pp \rightarrow t\bar{t}H$ *process, one important Higgs-production process at the LHC and considering the decay* $H \rightarrow b\bar{b}$ *,we compare these results to the potential background processes* $pp \rightarrow t\bar{t}Z$, $Z \rightarrow b\bar{b}$ *and* $pp \rightarrow t\bar{t}b\bar{b}$.

* National Technical University of Athens, School of Applied Mathematics & Physics

I. INTRODUCTION

1.MOTIVATION

The LHC is expected to provide answers for a number of major questions in today's physics. One of them is the search for the Higgs boson , which is believed to be the key to our understanding of the origin of mass as well as the proof of the non-trivial structure of vacuum. Moreover, since the Higgs mechanism constitutes a cornerstone of the Standard Model and its supersymmetric extensions, the existence of the Higgs boson would be a strong indication of its validity.

From a theoretical point of view, the Higgs mass is an arbitrary parameter, and once it is mesured, the couplings of the Higgs boson are also determined. So far, only some mass bounds have been estimated. For the possible Higgs mass range of 114-130 GeV/ c^2 an important Higgs production channel would be $pp \to t\bar{t}H$ with the gluon fusion as the dominant subprocess. The Higgs boson decay to $b\bar{b}$ would be the dominant mode (~85%) for the Higgs mass range up to 135 GeV/ c^2 .It would be therefore interesting to study the potential background processes $pp \to t\bar{t}Z\,,\, Z \to b\bar{b}$ and $pp \to t\bar{t}b\bar{b}$ so as to compare the results with the Higgs- production process. It is essential to point out that in this report we do not consider any t-quark decays.

In fact, the study of heavy quarks is also a significant goal of physics at the LHC , where for an integrated Luminosity of $10^{34} cm^{-2} s^{-1}$, ~ 8 million $t\bar{t}$ and $10^{12} b\bar{b}$ events are expected per year, mainly via gluon fusion and quark-antiquark annihilation.These $t\bar{t}$ -pair production processes will constitute the greatest percentage of the t-quark production mechanisms at the LHC. For this reason, some calculations for the $pp \to t\bar{t}$ and $pp \to t\bar{t}\,jet$ processes are also presented in this report. In order to examine the dependence of the cross section on the factorization scale Q , some cross section calculations at different energy scales are also performed.

2. THEORETICAL BACKGROUND: ABOUT THE QCD IMPROVED PARTON MODEL

The high-energy interactions of hadrons are described by the QCD improved parton model.In this model, a hard-scattering process between two hadrons is the result of an interaction between the quarks and gluons which are the constituents of the incoming hadrons. The quark and gluon constituents of hadrons act as quasi-free particles (partons). The incoming hadrons provide “broad-band” beams of partons which posses varying fractions of the momenta of their parent hadrons. In fact, the incoming beams have a spectrum of longitudinal momenta determined by the parton distribution functions. The centre of mass of the parton-parton scattering is normally boosted with respect to that of the two incoming hadrons. Thus, the final state is defined in terms of variables which transform simply under longitudinal boosts. We therefore introduce the rapidity y ,the transverse momentum P_T and the azimuthal angle ϕ . In terms of these variables, the four-momentum of a particle of mass m may be written as

$$p^{\mu} = (E, p_x, p_y, p_z) = (m_T \cosh y,\ P_T \sin\phi,\ m_T \sinh y)$$

where the transverse mass is defined as

$m_T = \sqrt{p_T^2 + m^2}$ and the rapidity is defined by $y = \frac{1}{2} \ln \frac{(E + p_z)}{(E - p_z)}$.

Rapidity differences are boost invariant.

In practice, the rapidity is often replaced by the pseudorapidity η , ($\eta \equiv -\ln \tan(\theta/2)$)which coincides with the rapidity in the $m \to 0$ limit. It is also common to use the transverse energy $E_T \equiv E \sin\theta$ rather than the transverse momentum .

Attempting to free a quark produces a jet of hadrons through production of quark -antiquark pairs and gluons. A jet could be described as a colorless, collimated bundle of particles . Many methods can be used to define what is meant by a jet of hadrons. One can use a cone algorithm based on the energy deposition in an angular region or a clustering algorithm based on combining particle momenta. For hadron-hadron collisions, the most commonly-used definition is

of the cone-type: a jet is a concentration of transverse energy in a 'cone' of radius R where $R=\sqrt{(\Delta\eta^2+\Delta\phi^2)}$. In defining R in terms of $\Delta\eta$ we obtain a jet measure invariant under longitudinal boosts. In the 2-dimensional η, ϕ plane, curves of constant R are circles around the axis of the jet. The precise value of a jet cross section depends on the jet definition . The cone size R can be varied and the measured jet cross section wil depend on the value chosen . In particular, the cross section increases when the cone is enlarged. Thus, a standard cone algorithm has been proposed , in which the trensverse energy, pseudoprapidity and azimuth of the jet are calculated by performing energy weighted sums over the particles contained within a cone of radius R : $E_T=\sum_{i\in R} E_T(i)$, $\eta_{jet}=\frac{1}{E_T}\sum_{i\in R} E_T(i)\eta(i)$, $\phi_{jet}=\frac{1}{E_T}\sum_{i\in R} E_T(i)\phi(i)$ .In this standard algorithm, the choice R = 0.7 is recommended.

The cross section for a hard scattering process initiated by two hadrons with four-momenta P_1, P_2 can be writen as:

$$\sigma(P_1, P_2)=\sum_{ij}\int dx_1\, dx_2\, f_i(x_1, \mu^2) f_j(x_2, \mu^2)\hat{\sigma}_{ij}(p_1, p_2, \alpha_S(\mu^2), Q^2/\mu^2)$$

The momenta of the partons which participate in the hard interaction are $p_1=x_1P_1$ and $p_2=x_2P_2$. The characteristic scale of the hard scattering is denoted by Q. As Q we could define e.g. the mass of a heavy quark or a weak boson, or the transverse momentum of a jet. The functions $f_i(x,\mu^2)$ are the QCD quark/gluon distributions, defined at a factorizaton scale μ .The short-distance cross-section for the scattering of partons of types i and j is denoted by $\hat{\sigma}_{ij}$. Because the coupling is small at high-energy, the short-distance cross section can be calculated as a perurbation series in the running coupling α_s .In higher orders, the short-distance cross section is derived from the parton scattering cross section by removing long distance pieces and factoring them into the parton distribution functions, which is necessary because the pertubatively calculated cross section contains contributions from interactions which occur long before the hard scattering. These contributions can be factored out and absorbed into the description of the incoming hadrons. The remaining cross section involves only high momentum transfers (short times and distances) and is insensitive to the physics of low momentum scales. The short-distance cross sections does not depend on the details of the hadron wave function or the type of the incoming hadron, it is a purely short-distance construct and is calculable in perturbation theory because of asymmptotic freedom.This factorization property of the cross section can be proved to all orders in perturbation theory and consists a fundamental property of the theory which turns QCD into a reliable calculational tool.

In the leading approximation ,however, at which the calculations for this report are performed, the short-distance cross section is identical to the normal parton scattering cross section calculated as a cross section for a QED process.

The factorizaton scale μ is an arbitrary parameter and it could be described as the scale which seperates the long- and short- distance physics. Thus a parton emitted with a small tranverse momentum, less than the scale μ ,is considered part of the hadron srtucture and is absorbed into the parton distribution. On the contrary, a parton emitted at large transverse momentum is part of the short-distance cross section. The scale μ should be chosen to be of the order of the hard scale Q which characterizes the parton-parton interaction. The standard choice is $\mu\equiv Q$.

II. METHOD

For the cross section calculations as well as for the plots, we used Madevent, a multi- purpose , tree -level event generator powered by the matrix element creator Madgraph. Madgraph identifies and plots Feynman Diagrams and creates a FORTRAN-77 code -which is compilled using the g77 compiler under LINUX- for the matrix element squared. It can handle tree-level processes with many particles in the final state and it maintains full spin correlations/ interference.

Madevent uses the Madgraph output and diagram information to automatically build an efficient phase space

integration and packages it in a process-dependent , self-contained Monte Carlo package for cross section evaluation and event generation. The code is generated for a specific simulation in the Standard Model or beyond and at any collider upon user's request.

Given the process, Madgraph automatically creates the amplitudes for all the relevant subprocesses and produces the mappings for the integration over the phase space . This process-dependent information is packaged into Madevent . For each process we downloaded the code -which is self-contained and therefore needs no external library- and let it run over the PC so as to calculate the desired cross sections.

Once the events have been generated, event information (e.g. Particle id's , momenta, spin, color connections) is stored in the “Les Houches Event Files” (LHEF)format , may be passed directly to a Shower Monte Carlo Program (interface available for PYTHIA) or be used as inputs for combined matrix-element shower calculations. It is also possible to create a series of standard plots (as well as a root file containing the parton-level events) over the web. For this ,the Plotting Interface/ ExRoot Analysis tool has been used to create plots for the weighted events.

All of the calculations in this report were made in the Standard Model and optimised to the LHC Energy (14 TeV) and Luminosity($10^{34} cm^{-2} s^{-1}$). The parton distribution function used is CTEQ6L1 . The Higgs mass value was attributed to **1**20 GeV/ c^2 . Various characteristic scales were used($Q \equiv \{ m_Z, m_t, 2m_t, m_t/2 \}$). For each process, the Monte Carlo program created 10000 events. Finally, it is important to note that all calculations were performed at Leading Order .

III. RESULTS

1. THE $pp \to t\bar{t}$ PROCESS AND SUBPROCESSES

	CROSS SECTION σ (pb)	STATISTICAL ERROR (pb)	RELATIVE CONTRIBUTION %	# F.D.
$pp \to t\bar{t}$	751.1	2.9		5
$g\,g \to t\bar{t}$	660.2	2.9	87.9	3
$u\bar{u} \to t\bar{t}$ *	45.7	0.4	6.1	1
$\bar{u}u \to t\bar{t}$ **	45.2	0.4	6.0	1

In each of the cases * and ** the contributions from quarks of different flavours are included. The cross sections of these subprocesses for case * in particular have been independently calculated and they are presented in the following table:

	CROSS SECTION σ (pb)	RELATIVE CONTRIBUTION (to the total cross section) %
SUBPROCESSES		
$u\bar{u} \to t\bar{t}$	25.9	3.45
$d\bar{d} \to t\bar{t}$	16.3	2.17
$b\bar{b} \to t\bar{t}$	0.4	0.05
$s\bar{s} \to t\bar{t}$	2.7	0.36
$c\bar{c} \to t\bar{t}$	1.2	0.16

The main cross section contribution comes from the gluons .The valence quarks u and d have a considerable contribution as well. The contribution from the sea quarks b,s and c is very small.
Note that all the above results are for pure QCD processes (QED contributions set to zero) and for $Q \equiv m_Z$.

FEYNMAN DIAGRAMS

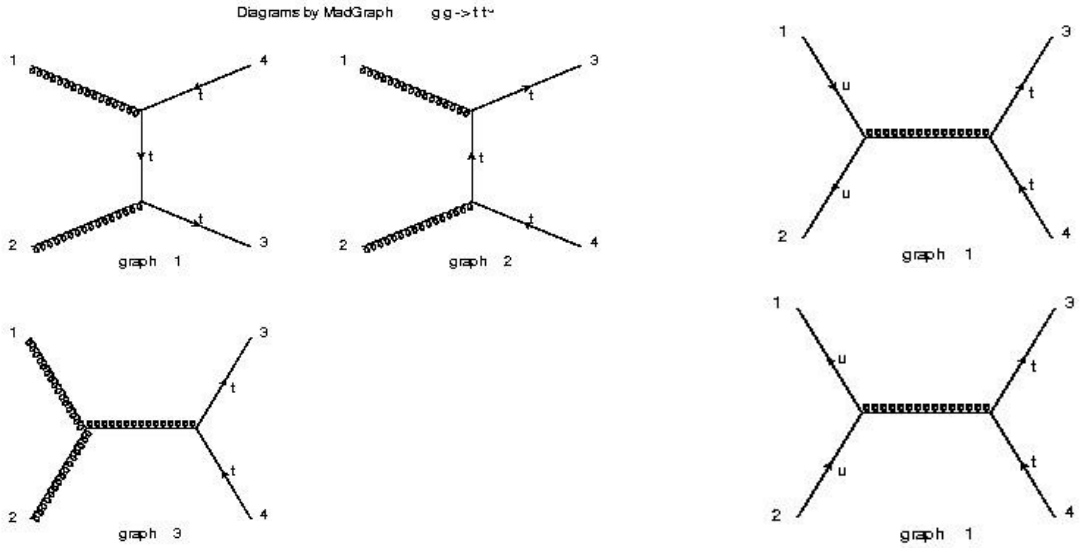

2. THE $pp \to t\,\bar{t}\,jet$ PROCESS AND SUBPROCESSES

	CROSS SECTION σ (pb)	STATISTICAL ERROR (pb)	RELATIVE CONTRIBUTION %	# F.D.
$pp \to t\,\bar{t}\,jet$	742.3	2.8		48
$g\,g \to t\,\bar{t}\,g$	578.0	2.1	77.9	18
$g\,u \to t\,\bar{t}\,u$	50.8	0.8	6.8	5
$u\,g \to t\,\bar{t}\,u$	50.8	0.6	6.8	5
$\bar{u}\,g \to t\,\bar{t}\,\bar{u}$	16.1	0.3	2.2	5
$g\,\bar{u} \to t\,\bar{t}\,\bar{u}$	15.8	0.4	2.1	5
$u\,\bar{u} \to t\,\bar{t}\,g$ *	15.5	0.2	2.1	5
$\bar{u}\,u \to t\,\bar{t}\,g$	15.4	0.3	2.1	5

Note that the main cross section contribution is coming from the gluon - gluon fusion. In this jet-producing process however, the gluon contribution is smaller than in the previous case.
In the following table the contributions of the subprocesses to the process -type * are presented

	CROSS SECTION σ (pb)	RELATIVE CONTRIBUTION % (to the total cross section)
SUBPROCESSES		
$u\,\bar{u} \to t\,\bar{t}\,jet$	8.7	1.17
$d\,\bar{d} \to t\,\bar{t}\,jet$	5.6	0.75
$b\,\bar{b} \to t\,\bar{t}\,jet$	0.1	0.01
$s\,\bar{s} \to t\,\bar{t}\,jet$	0.8	0.11
$c\,\bar{c} \to t\,\bar{t}\,jet$	0.3	0.04

FEYNMAN DIAGRAMS FOR $g\,g \to t\,\bar{t}\,g$

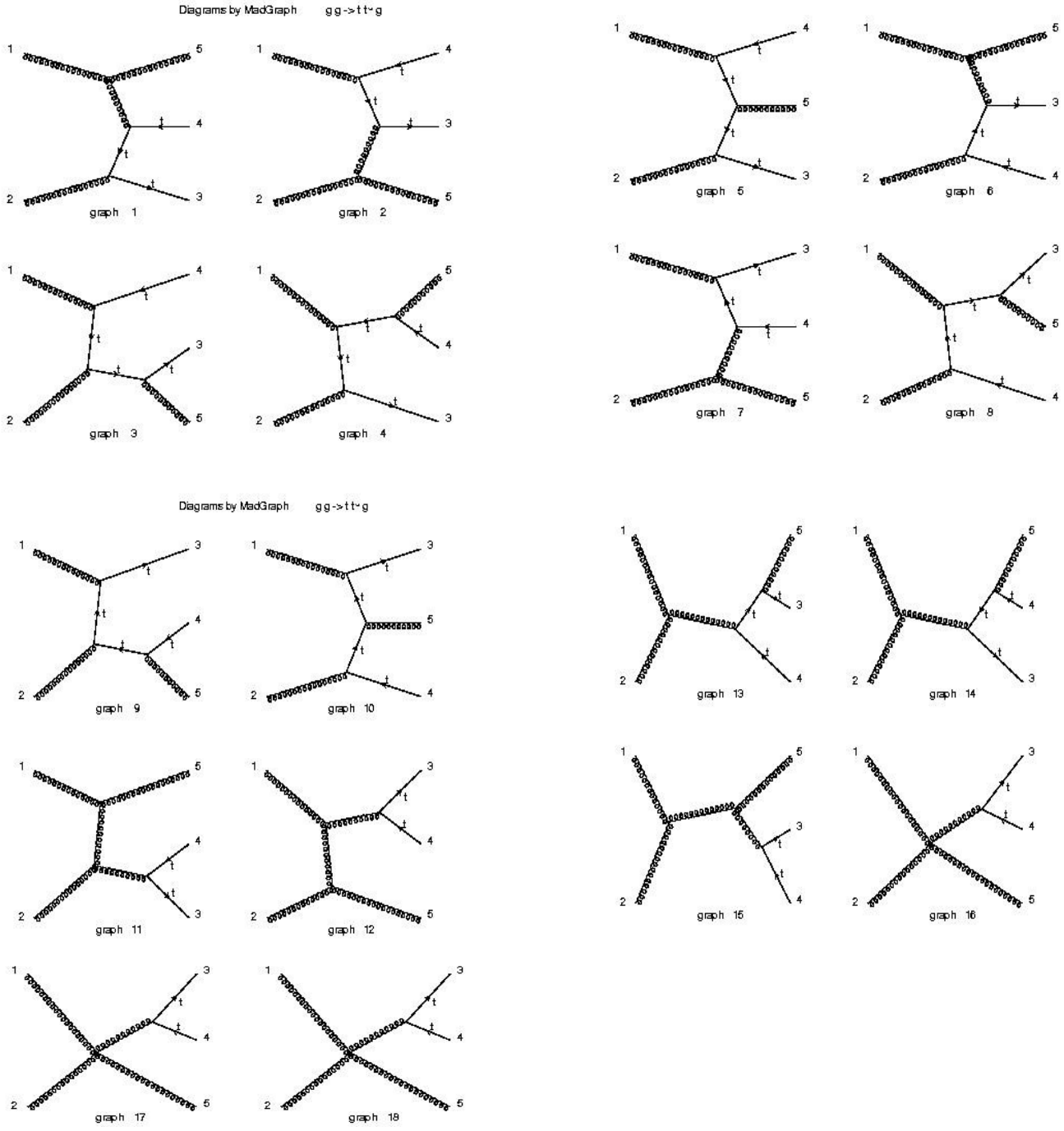

3. HISTOGRAMS FOR $pp \to t\,\bar{t}$ AND $pp \to t\,\bar{t}\,jet$

In order to illustrate the kinematic and dynamic effect of the jet, the histograms are compared:

$pp \to t\,\bar{t}$

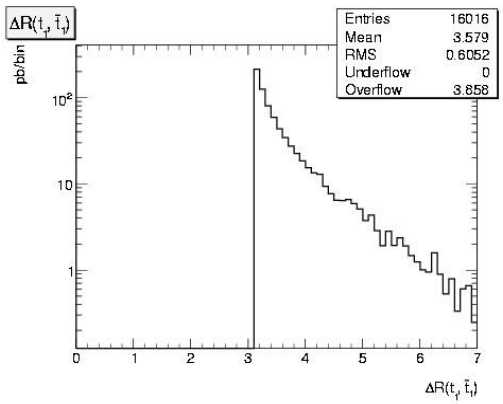

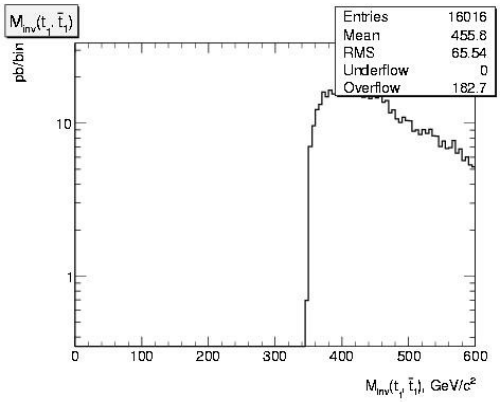

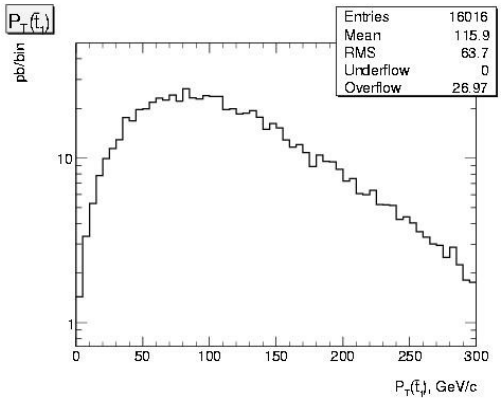

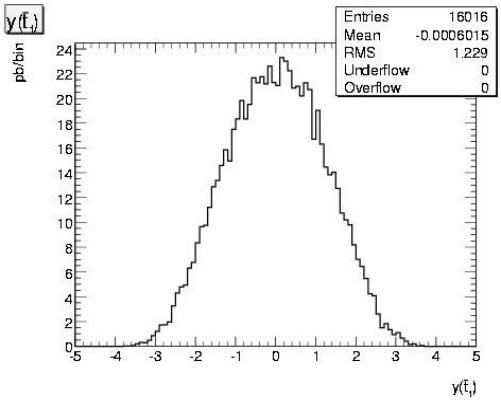

$pp \to t\,\bar{t}\;jet$

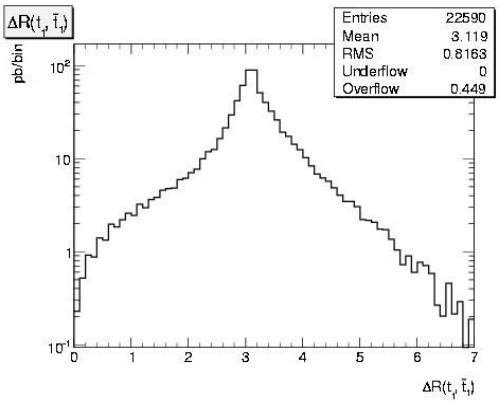

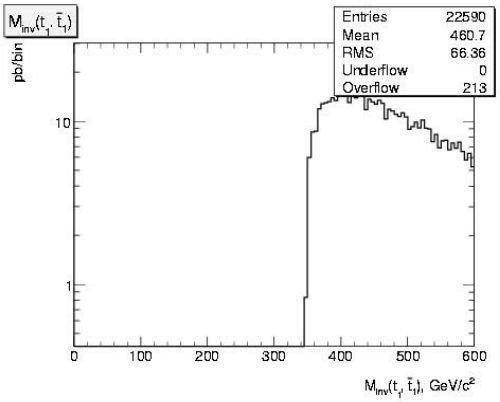

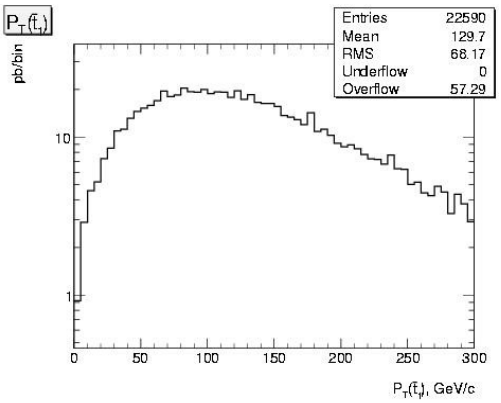

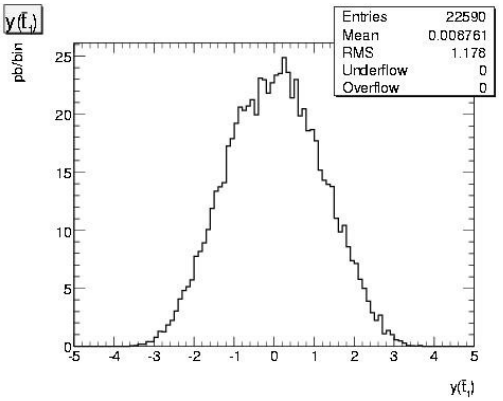

The plots for the t quark are identical (with only some small variations of statistical nature) to the ones for the $\bar{t}$, and thus they are ommited.

4. ADDITIONAL PLOTS FOR THE $pp \to t\,\bar{t}\,jet$ PROCESS:

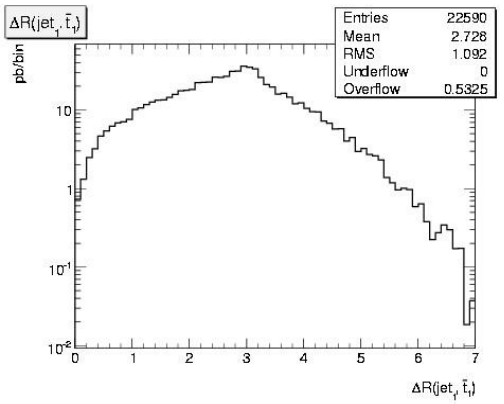

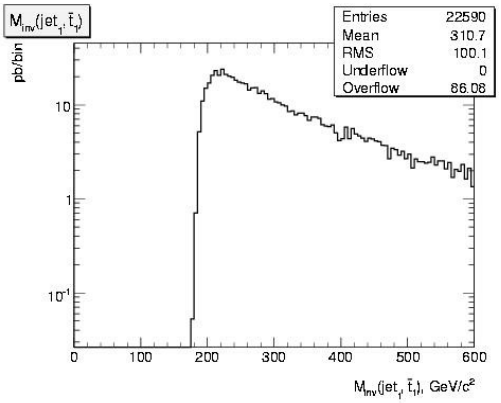

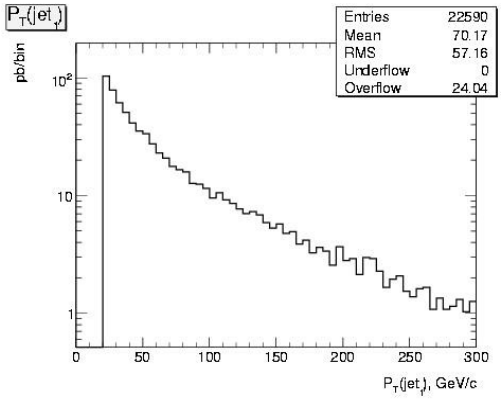

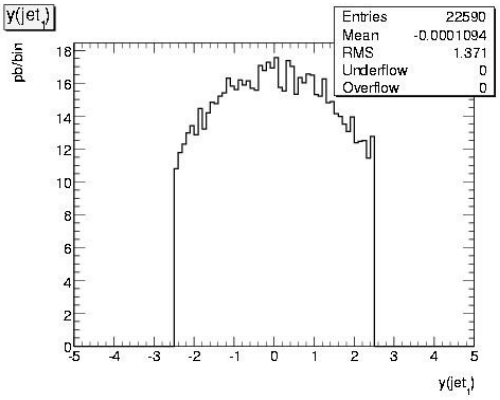

5. THE $pp \to t\,\bar{t}\,b\,\bar{b}$ PROCESS

	CROSS SECTION σ (pb)	STATISTICAL ERROR (pb)	RELATIVE CONTRIBUTION %	# F.D
$pp \to t\,\bar{t}\,b\,\bar{b}$	19.38	0.05		52
$g\,g \to t\,\bar{t}\,b\,\bar{b}$	18.38	0.05	94.8	38
$u\,\bar{u} \to t\,\bar{t}\,b\,\bar{b}$	0.50	0.01	2.6	7
$u\,\bar{u} \to t\,\bar{t}\,b\,\bar{b}$	0.50	0.01	2.6	7

In this case as well, there are of course contributions from the subprocesses with the valence quark d and the sea quarks s,c,b (the t -quark is too heavy to contribute) as initial particles in each process-type. These results, however are not presented here in detail.

Diagrams by MadGraph g g -> t t~ b b~

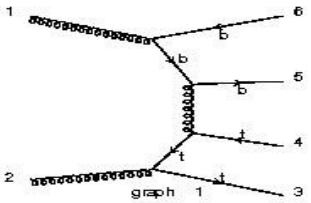

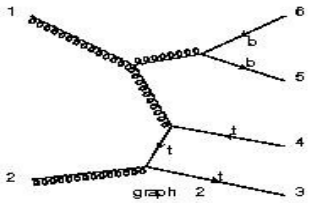

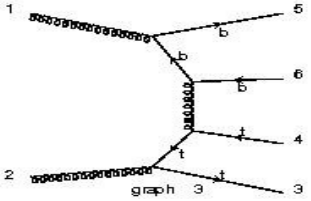

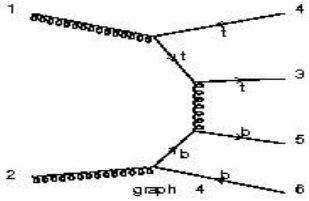

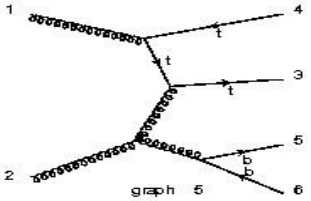

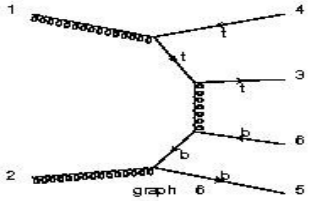

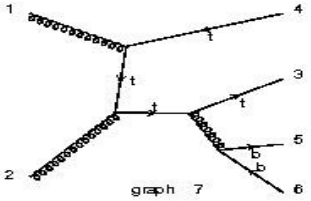

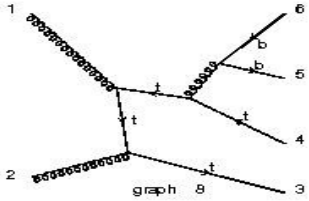

Diagrams by MadGraph g g -> t t~ b b~

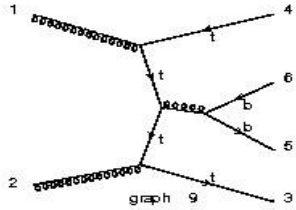

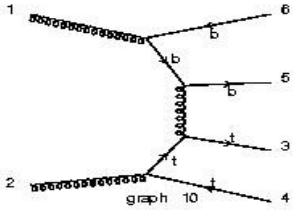

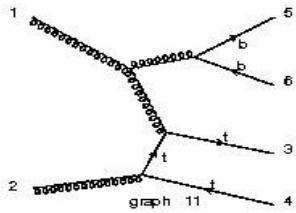

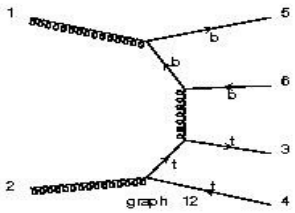

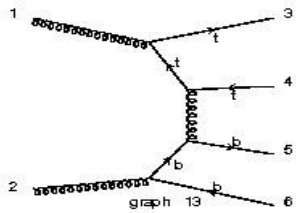

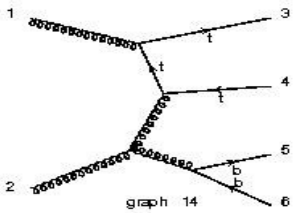

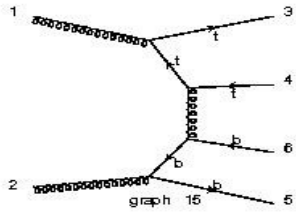

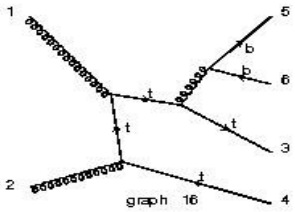

Diagrams by MadGraph g g -> t t~ b b~

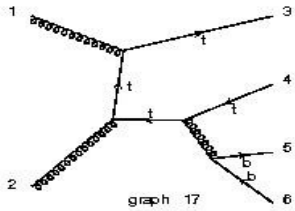

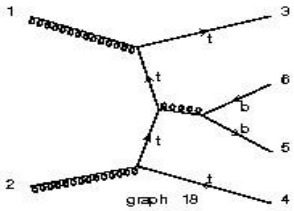

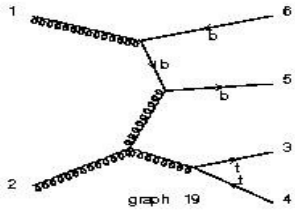

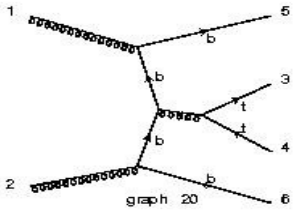

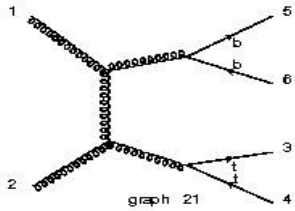

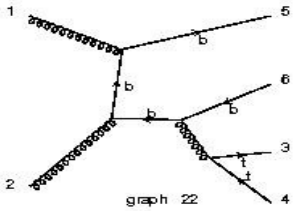

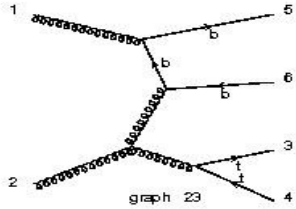

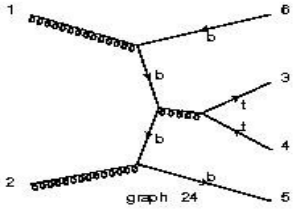

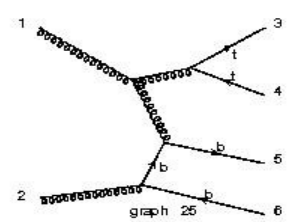

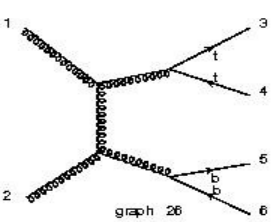

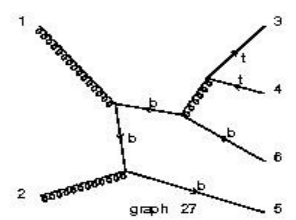

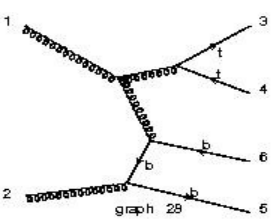

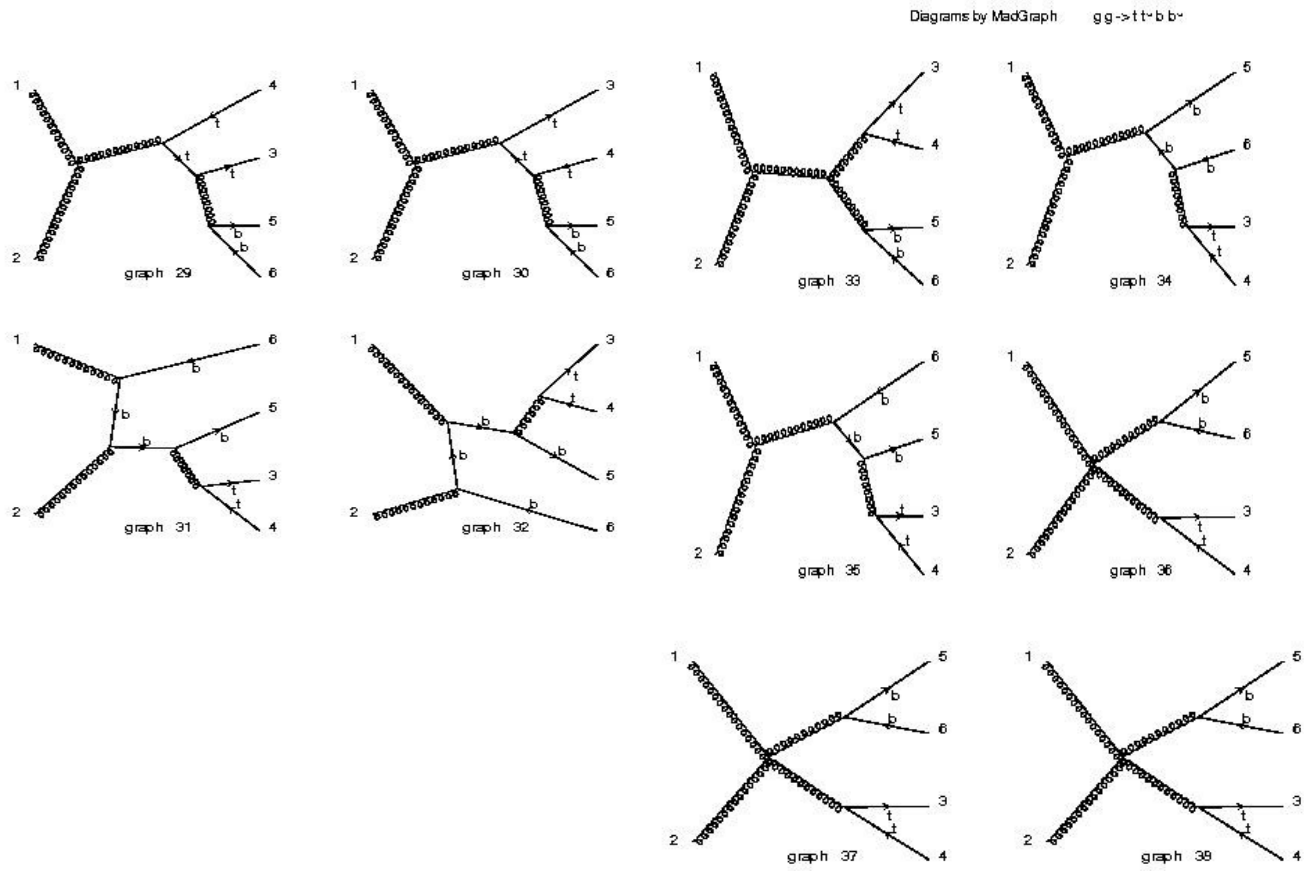

6. CROSS SECTION VARIATION WITH THE FACTORIZATION SCALE

The values of the cross sections for the previous processes and for their dominant gluon subprocesses are presented below for four different factorization scales .

CROSS SECTIONS (pb)	$m_t/2$	$m_Z = 91.2\,GeV$	$m_t = 170.9\,GeV$	$2\,m_t$
$pp \to t\,\bar{t}$	772.6	751.1	585.7	454.4
$g\,g \to t\,\bar{t}$	680.8	660.2	508.8	387.7
$pp \to t\,\bar{t}\;jet$	773.3	742.3	517.1	356.4
$g\,g \to t\,\bar{t}\;jet$	605.4	578.0	401.0	271.4
$pp \to t\,\bar{t}\,b\,\bar{b}$	20.3	19.4	12.0	7.4
$g\,g \to t\,\bar{t}\,b\,\bar{b}$	19.3	18.4	11.4	7.0

In order to illustrate the dependence of the parton distribution function on the factorization scale, the following diagrams generated by HEPDATA are presented:

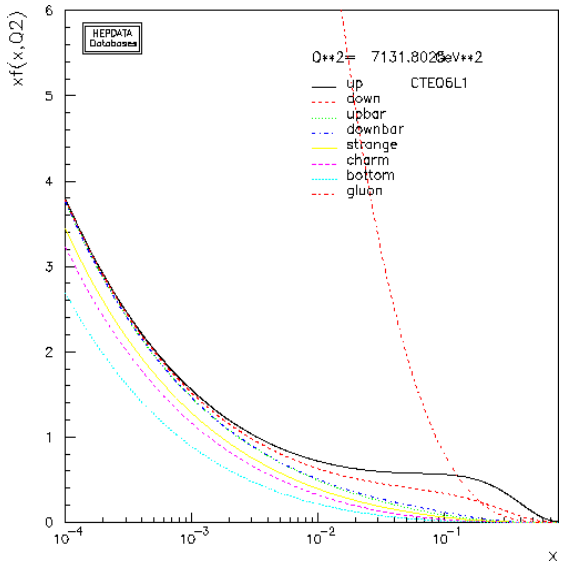

Q=m(t)/2

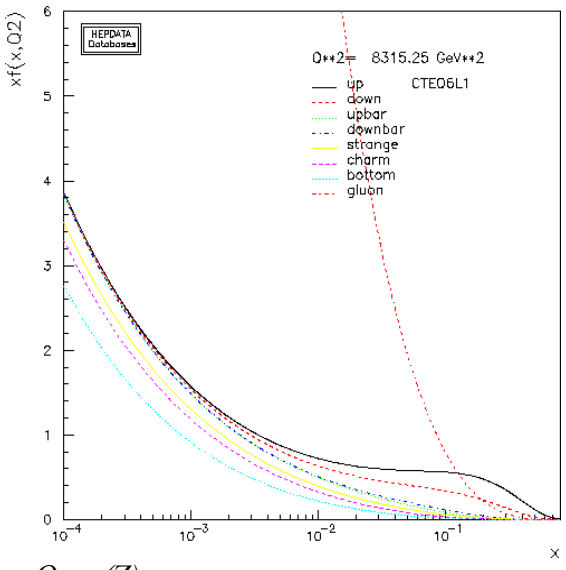

Q=m(Z)

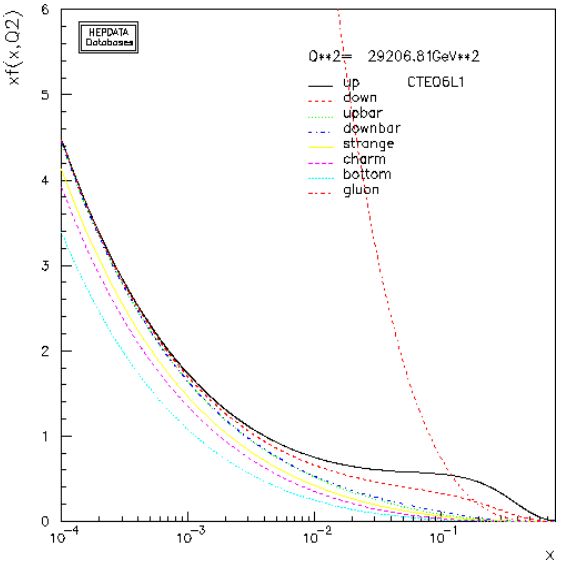

Q=m(t)

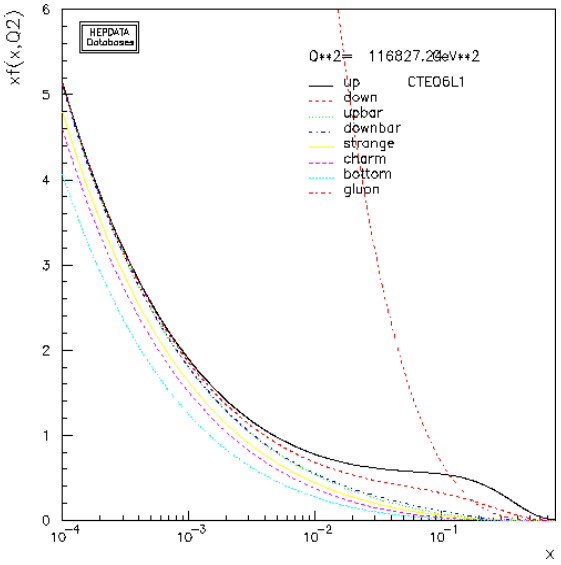

Q=2 m(t)

7. THE $pp \to t\,\bar{t}\,H$ PROCESS

For the energy scale $Q \equiv m_Z$ and having considered both QED and QCD contributions , we got the following cross section results:

	CROSS SECTION σ (fb)	STATISTICAL ERROR (fb)	RELATIVE CONTRIBUTION %	# F.D.
$pp \to t\,\bar{t}\,H$	790.3	2.8		36
$g\,g \to t\,\bar{t}\,H$	560.6	2.2	70.9	8
$u\,\bar{u} \to t\,\bar{t}\,H$ *	69.3	1.0	8.8	7
$\bar{u}\,u \to t\,\bar{t}\,H$ *	68.0	0.9	8.6	7
$\bar{d}\,d \to t\,\bar{t}\,H$ **	46.3	0.6	5.9	7
$d\,\bar{d} \to t\,\bar{t}\,H$ **	46.1	0.6	5.8	7

In this case , Madgraph includes the contributions of the subprocesses with u and c quarks as initial particles to the * process-types and the contributions of the subprocesses with d and s quarks as initial particles to the ** process-types. Once again, the main contribution to the total cross section is coming from the gluon process.

FEYNMAN DIAGRAMS FOR $g\,g \to t\,\bar{t}\,H$

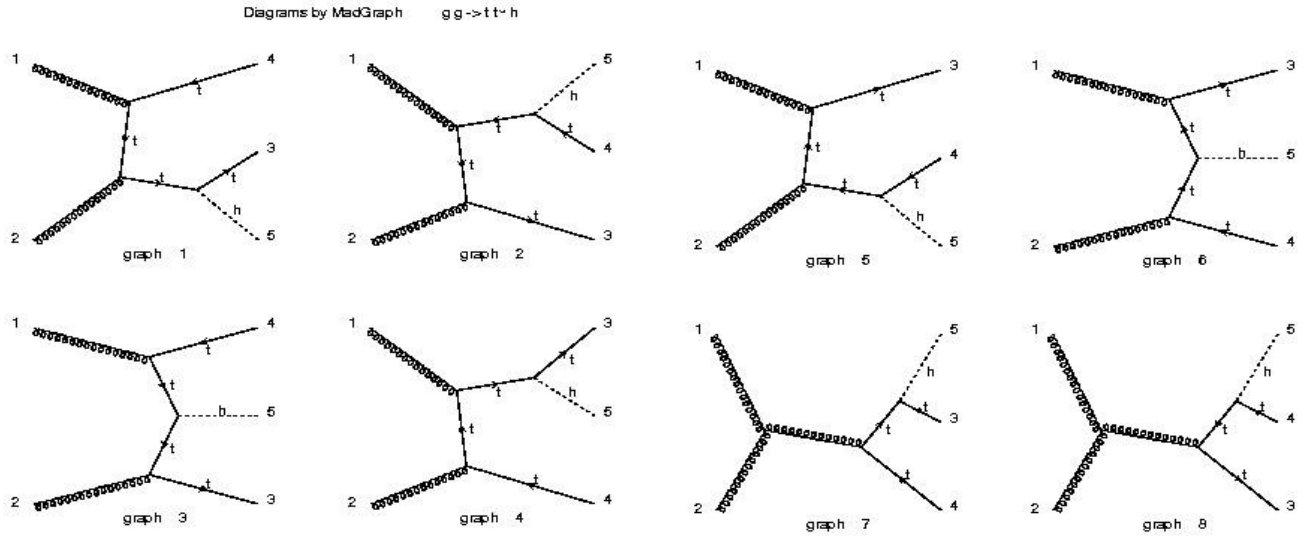

The histograms generated f or the $pp \to t\,\bar{t}\,H$ process are presented below:

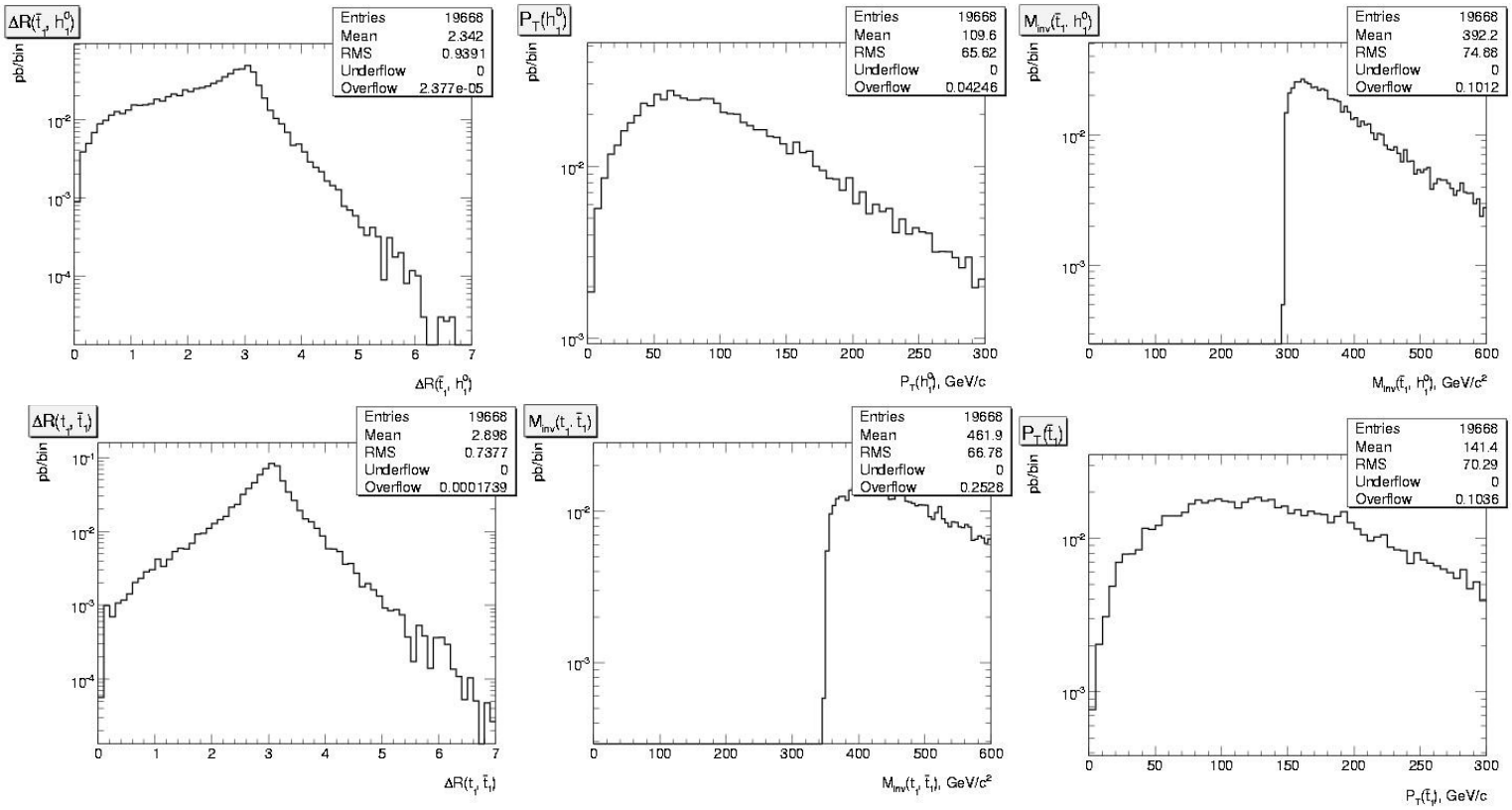

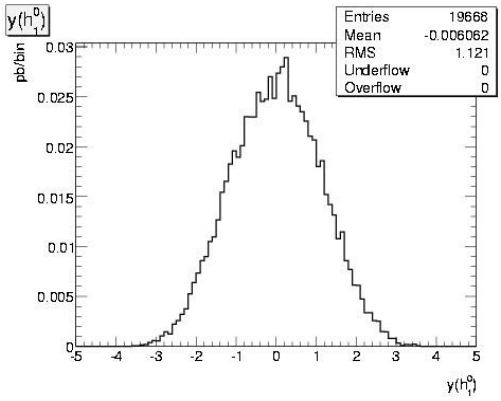

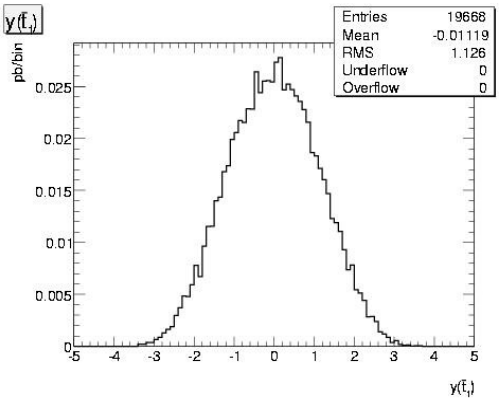

8. $pp \to t\,\bar{t}\,H$ AND BACKGROUND

The Higgs boson ,shortly after its production, is very likely to decay to $b\,\bar{b}$. Thus, it is useful to present the cross section results for its main background processes $pp \to t\,\bar{t}\,Z\,,\,Z \to b\,\bar{b}$ and $pp \to t\,\bar{t}\,b\,\bar{b}$. For reasons of completeness, in these calculations QED contributions are also taken into consideration.

	CROSS SECTION σ	STATISTICAL ERROR	RELATIVE CONTRIBUTION %	# F.D.
$pp \to t\,\bar{t}\,b\,\bar{b}$	20.33 pb	0.08 pb		470
$g\,g \to t\,\bar{t}\,b\,\bar{b}$	19.17 pb	0.06 pb	94.3	134
$u\,\bar{u} \to t\,\bar{t}\,b\,\bar{b}$	0.35 pb	0.01 pb	1.7	84
$\bar{u}\,u \to t\,\bar{t}\,b\,\bar{b}$	0.35 pb	0.01 pb	1.7	84
$\bar{d}\,d \to t\,\bar{t}\,b\,\bar{b}$	0.25 pb	0.01 pb	1.2	84
$d\,\bar{d} \to t\,\bar{t}\,b\,\bar{b}$	0.23 pb	0.01 pb	1.1	84

$pp \to t\,\bar{t}\,Z$	1018.9 fb	3.3 fb		60
$g\,g \to t\,\bar{t}\,Z$	685.5 fb	2.9 fb	67.3	8
$\bar{d}\,d \to t\,\bar{t}\,Z$	99.1 fb	0.8 fb	9.7	13
$d\,\bar{d} \to t\,\bar{t}\,Z$	98.9 fb	1.0 fb	9.7	13
$u\,\bar{u} \to t\,\bar{t}\,Z$	67.9 fb	0.7 fb	6.7	13
$\bar{u}\,u \to t\,\bar{t}\,Z$	67.5 fb	0.7 fb	6.6	13

Note that the branching ratio for the Higgs decay to $b\,\bar{b}$ is ~85%. and the branching ratio for the Z decay to $b\,\bar{b}$ is ~15.2 % . The cross sections of the Higgs -producing process and of the background processes, after having taken the decay proccesses into consideration, are summarised in the table below:

$pp \to t\,\bar{t}\,b\,\bar{b}$	CROSS SECTION σ	STATISTICAL ERROR	RELATIVE CONTRIBUTION %
$pp \to t\,\bar{t}\,b\,\bar{b}$ directly	20.33 pb	0.08 pb	96.1
$pp \to t\,\bar{t}\,Z\,,\,Z \to b\,\bar{b}$	154.9 fb	0.5 fb	0.7
$pp \to t\,\bar{t}\,H\,,\,H \to b\,\bar{b}$	671.8 fb	2.4 fb	3.2

Supposing that these are the only three dominant $t\,\bar{t}\,b\,\bar{b}$ production processes, the relative contribution of each process has also been calculated. The histograms of these three processes are compared below:

$pp \to t\bar{t}H, H \to b\bar{b}$

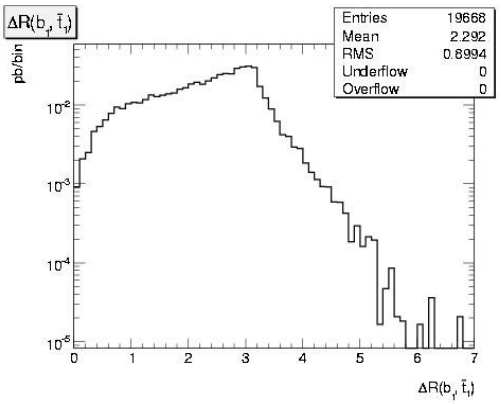

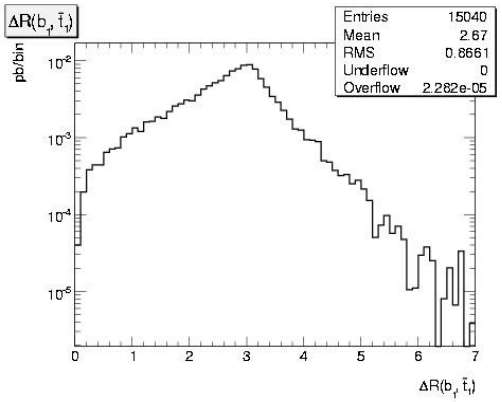

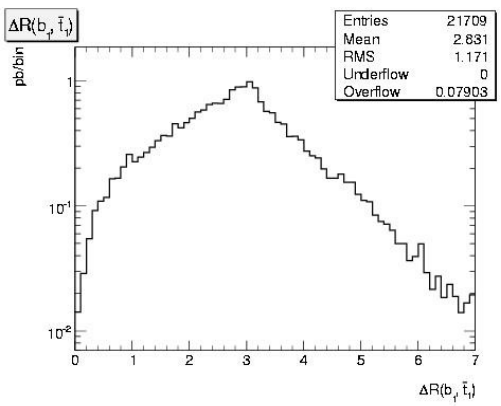

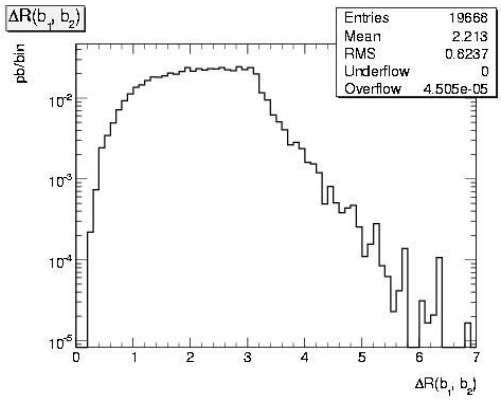

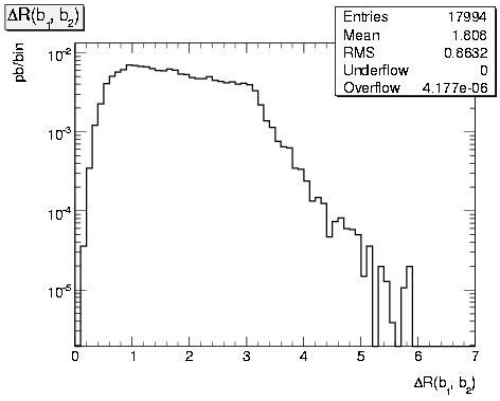

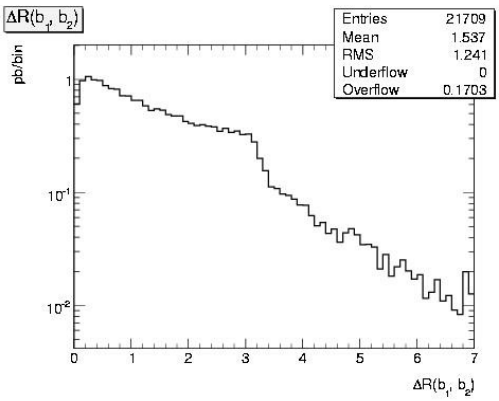

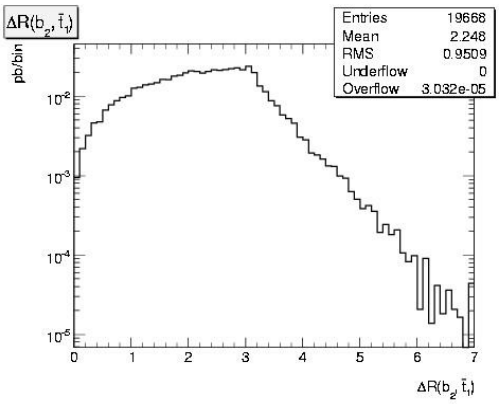

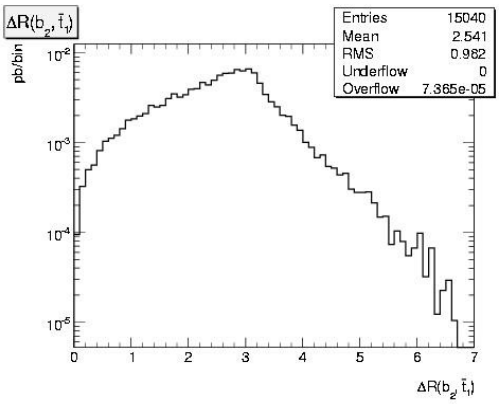

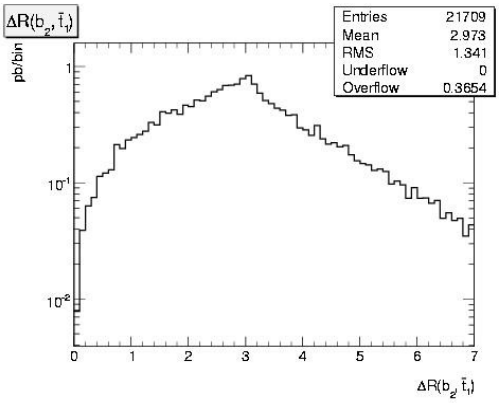

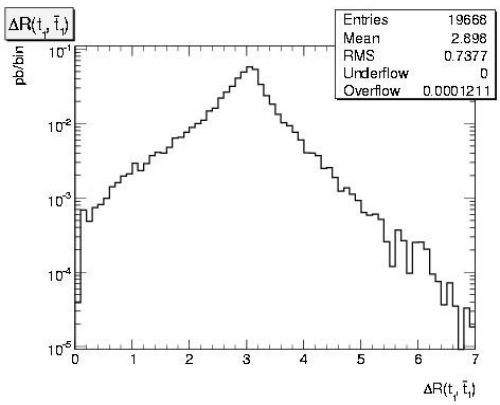

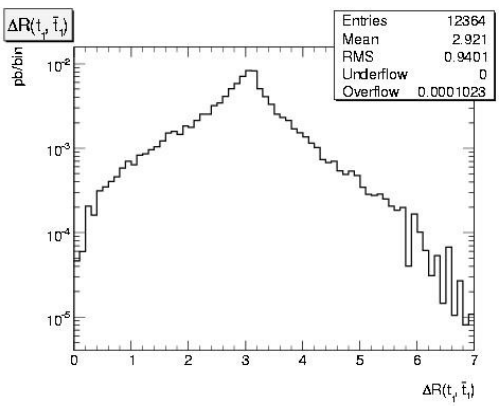

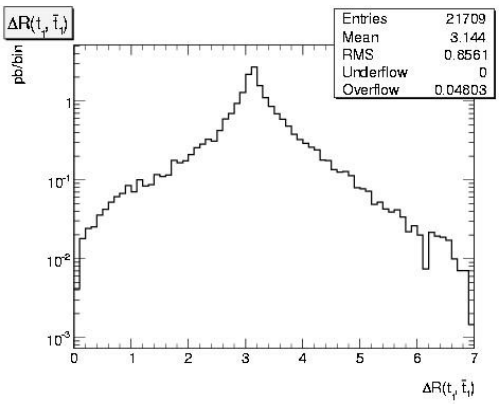

$pp \to t\bar{t}Z, Z \to b\bar{b}$

$pp \to t\bar{t}b\bar{b}$

$pp \to t\bar{t}H, H \to b\bar{b}$

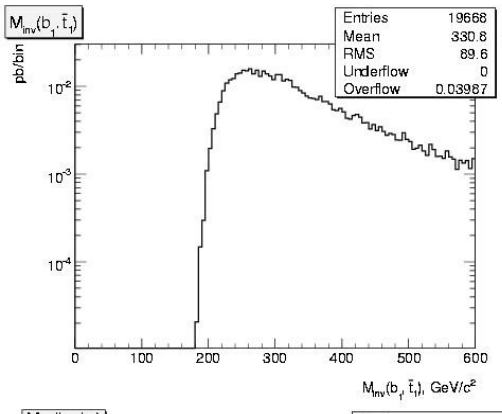

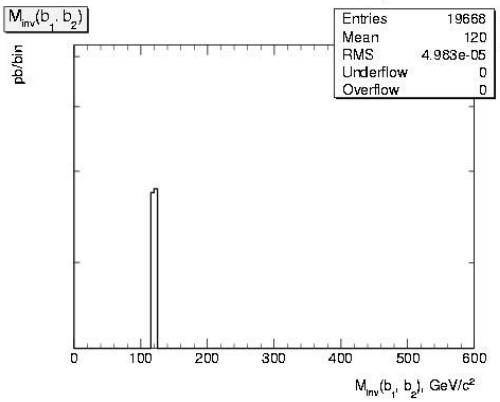

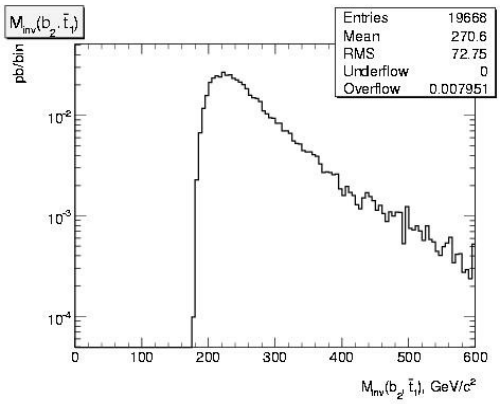

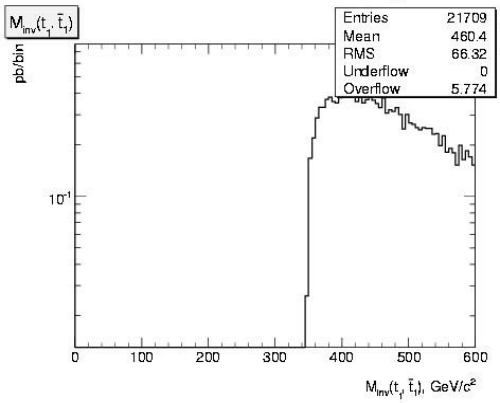

$pp \to t\bar{t}Z, Z \to b\bar{b}$

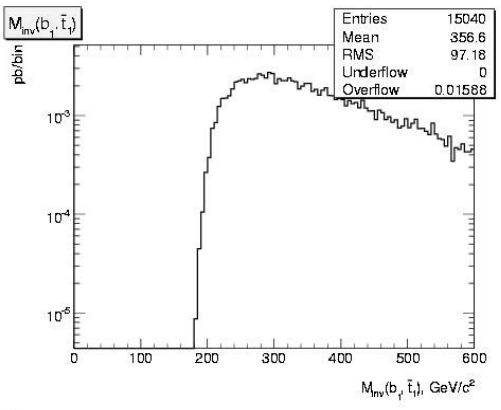

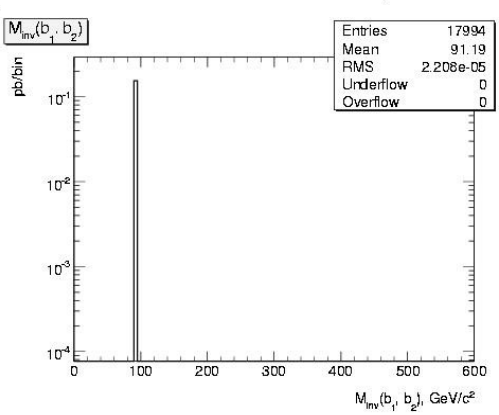

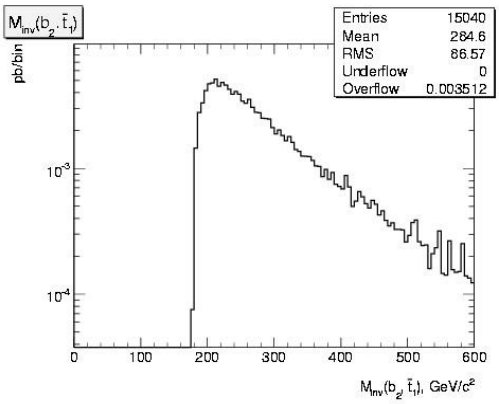

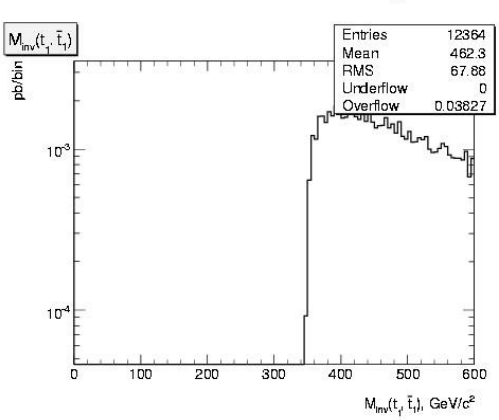

$pp \to t\bar{t}b\bar{b}$

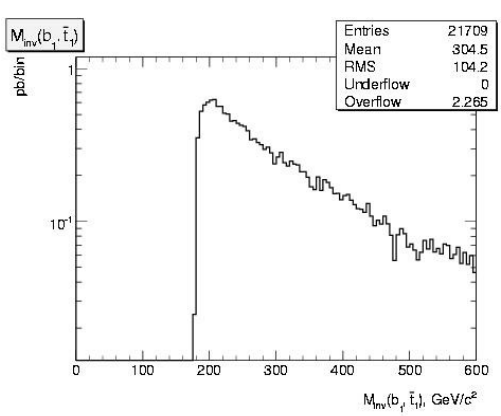

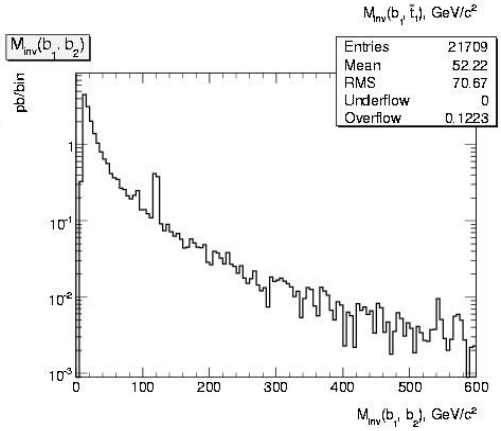

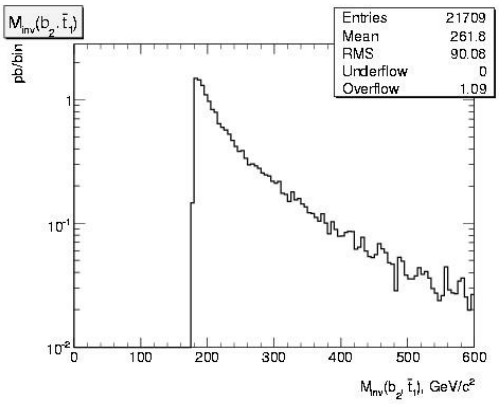

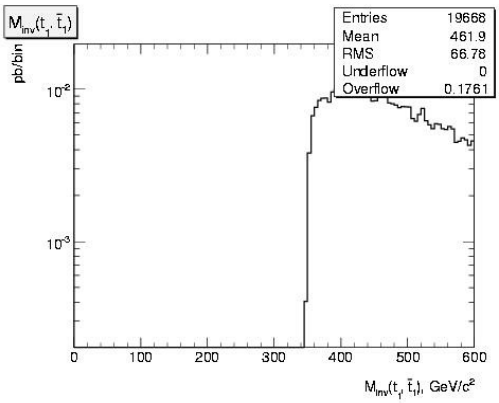

$pp \to t\bar{t}H, H \to b\bar{b}$

$pp \to t\bar{t}Z, Z \to b\bar{b}$

$pp \to t\bar{t}b\bar{b}$

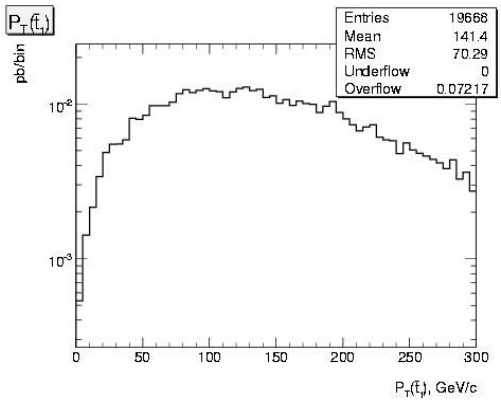

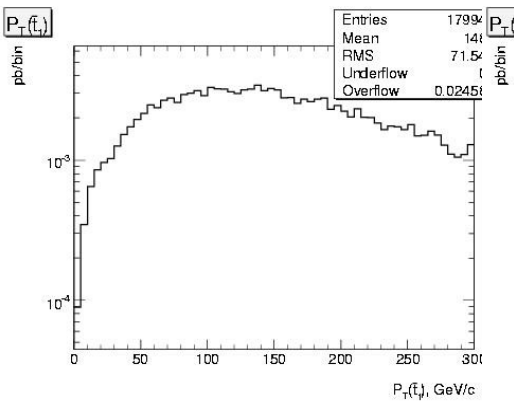

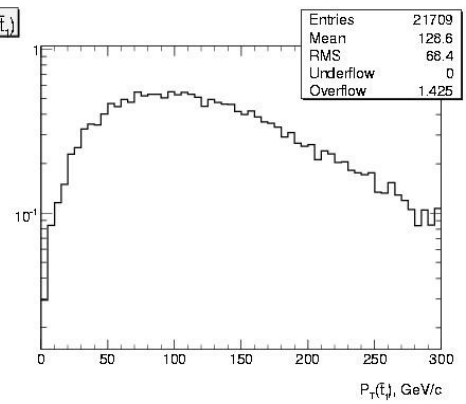

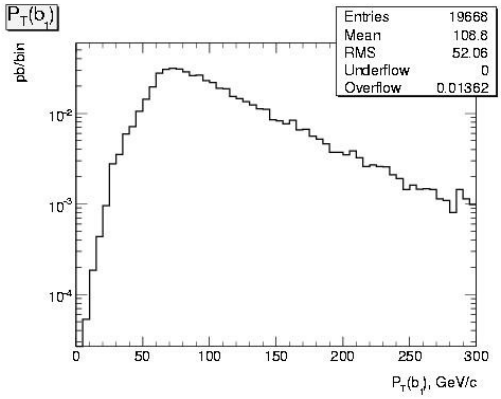

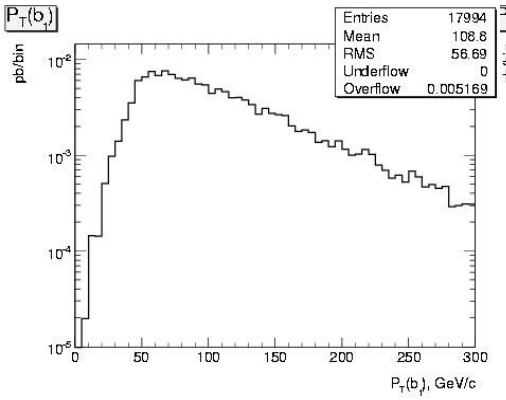

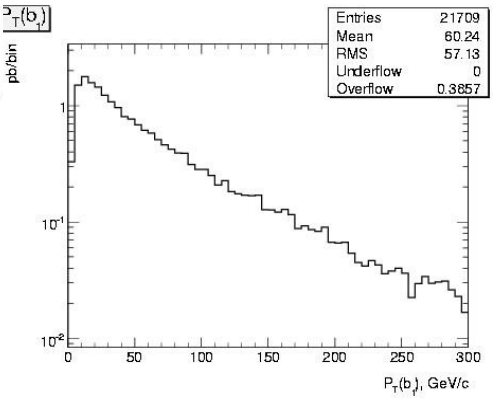

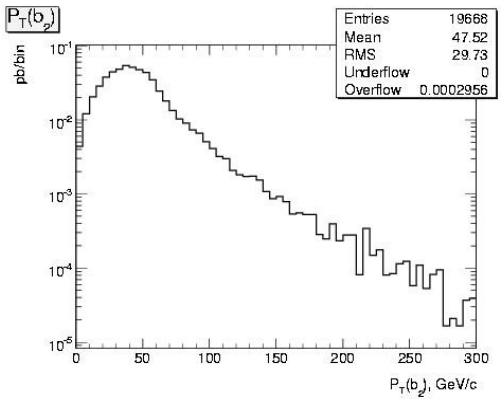

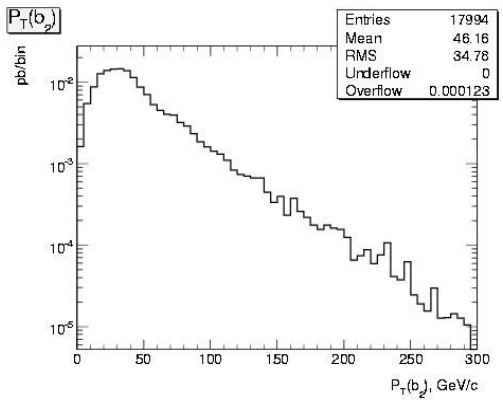

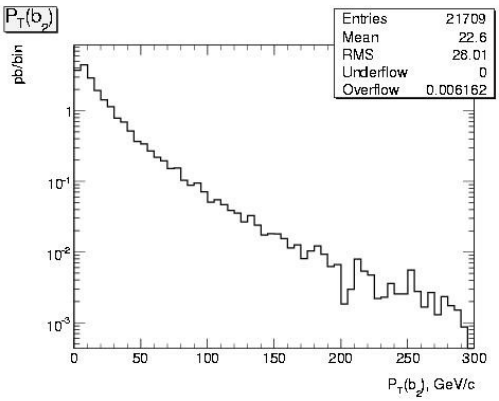

$pp \to t\bar{t}H, H \to b\bar{b}$

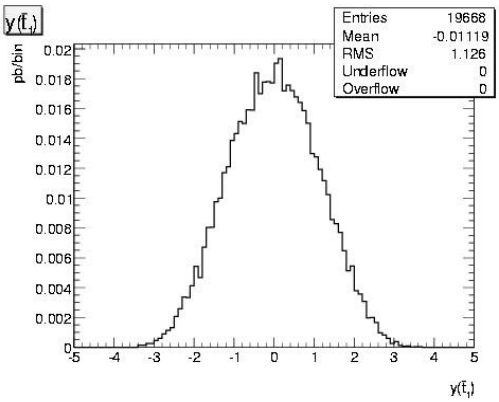

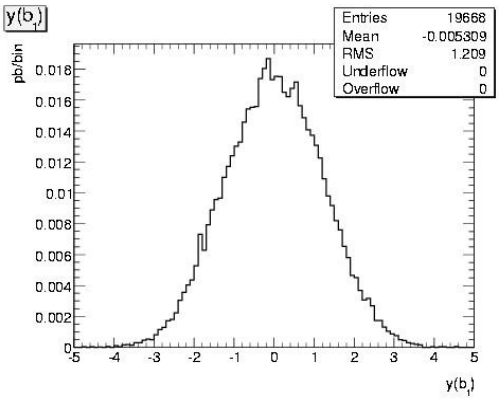

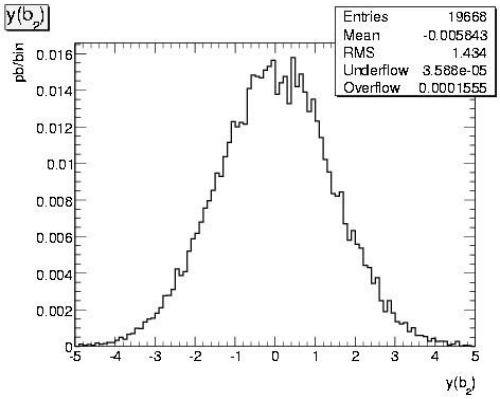

$pp \to t\bar{t}Z, Z \to b\bar{b}$

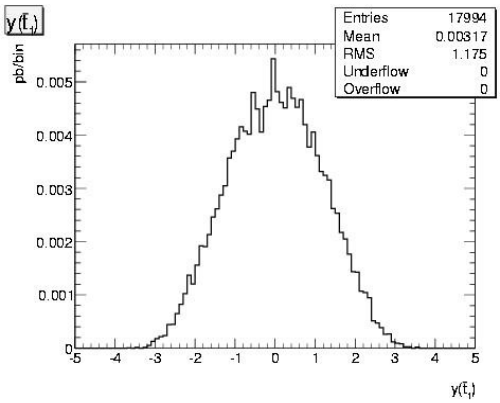

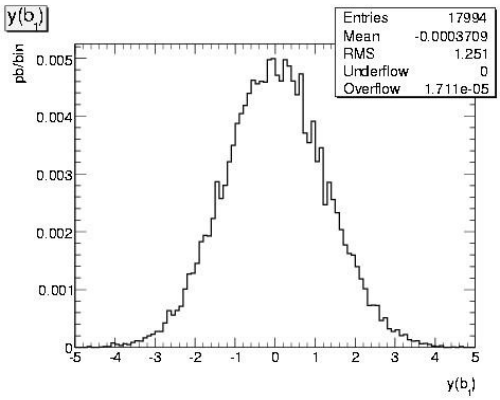

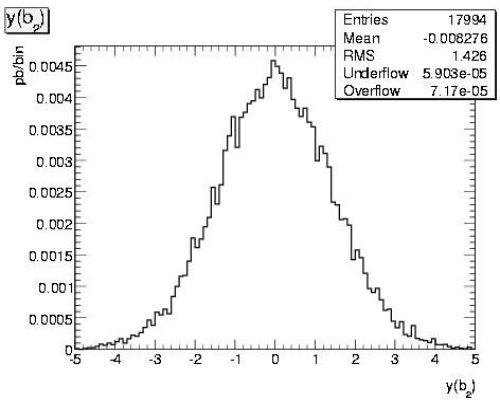

$pp \to t\bar{t}b\bar{b}$

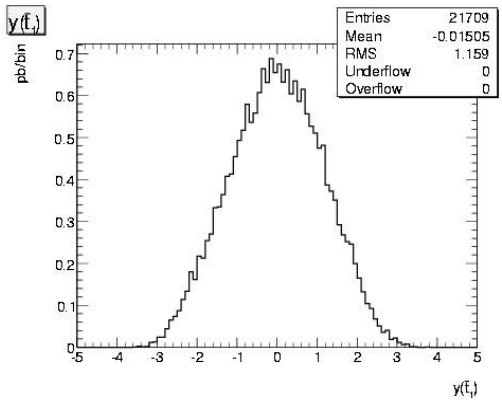

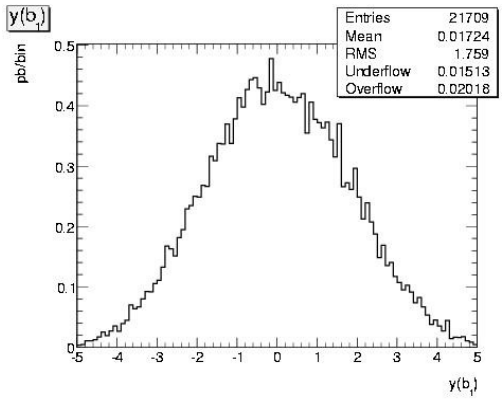

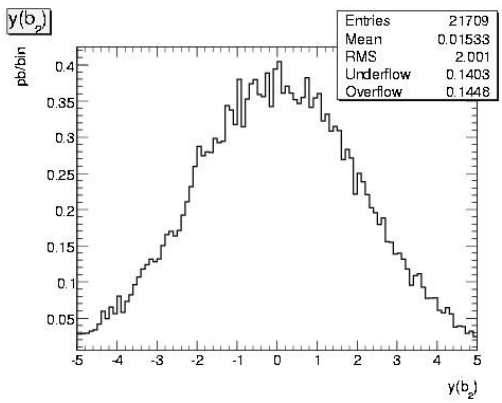

IV. CONCLUSION

Madgraph proved to be more than effective, both as a cross section calculator and as a plotting tool, as it gives the user a wide variety of input options and provides detailed results for the subprocesses. It therefore enables the user to process/ evaluate the information as needed .

We summarise some comments on the results presented in this report:
*I n all processes, the gluon fusion is the dominant subprocess, its relative contribution ,though, varies according to the process. In our results, the gluon fusion contribution covers a range of 67.3-94.8% . The contribution of the s,c,b -sea quarks is small ,but should also be taken into consideration .
*By compairing the histograms of $pp \to t\,\bar{t}$ and $pp \to t\,\bar{t}\,jet$,we deduce that the jet production does not differentiate significantly the distribution of the rapidity, the transverse momentum,or the invariant mass of $t\,,\,\bar{t}$ .The main differentiation, which is expected as it stems from the momentum conservation, is in the ΔR distribution.
*The cross section for the process $pp \to t\,\bar{t}\,b\,\bar{b}$ is ~5 % greater, if we include QED contributions .
*The dependency of the parton distribution function on the factorization scale can sufficiently explain the variation of the cross section according to the factorization scale, considering the cross section definition $\sigma(P_1, P_2) = \sum_{ij} \int dx_1\, dx_2\, f_i(x_1, \mu^2)\, f_j(x_2, \mu^2)\, \hat{\sigma}_{ij}(p_1, p_2, \alpha_S(\mu^2), Q^2/\mu^2)$
*Regarding the Higgs process, it is interesting to note that despite its small cross section compared to the background processes ,its high branching ratio for the $H \to b\,\bar{b}$ decay makes its contribution to the $t\,\bar{t}\,b\,\bar{b}$ final state-processes considerable(3.2%) .
*The ΔR histograms for the processes $pp \to t\,\bar{t}\,Z\,,\,Z \to b\,\bar{b}$ and $pp \to t\,\bar{t}\,H\,,\,H \to b\,\bar{b}$ are similar in shape, but can easily be distinguished ,since the scale is different . The scale for the $pp \to t\,\bar{t}\,b\,\bar{b}$ process is of course much bigger. Concerning the P_T histograms ,though, in the case of the Higgs process a higher scale is reached .Regarding the y histograms , the differentiation lies in the scales and in the fact that for the $t\,\bar{t}\,b\,\bar{b}$ process the b-quarks have a bigger range of possible rapidity values. Finally, the histograms of the invariant mass of the b-quarks are more interesting, since in the $pp \to t\,\bar{t}\,b\,\bar{b}$ process a mass distribution is given instead of a sharp edge as in the decay processes.

V. ACKNOWLEDGEMENTS

I would like to thank my supervisor Sven-Olaf Moch for giving me the opportunity to work on this interesting topic. I am also very grateful to Bas Tausk and Theodoros Diakonidis for their support on this project, Kouhei Hasegawa for his help with my computing questions, and last but not least, to all the DESY staff for the excellent cooperation.

VI. REFERENCES

(1) BOOKS

1. R.K. Ellis, W.J. Stirling & B.R. Webber, *QCD & Collider Physics*
2. R.D.Field, *Applications of Perturbative QCD*
3. M.E. Peskin, D.V. Schroeder, *An Introduction to Quantum Field Theory*
4. *ATLAS Detector + Physics Performance*- Technical Design Report-Volume II , 1999
5. *CMS Physics* -Technical Design Report -Volume II, 2006

(2) PAPERS

1.M.H. Seymour, *Quantum Chromodynamics* - arXiv:hep- ph/0505192 v1 23 May 2005

(3) WEBPAGES

1. http://madgraph.phys.ucl.ac.be
2. http://madgraph.roma2.infn.it
3. http://madgraph.hep.uiuc.edu
4. http://durpdg.dur.ac.uk/hepdata/pdf3.html